Quinone exchange at the A1 site in Photosystem I in spinach and cyanobacteria

ARTICLE *in* BIOCHIMICA ET BIOPHYSICA ACTA (BBA) - BIOENERGETICS · JUNE 1997

Impact Factor: 5.35 · DOI: 10.1016/S0005-2728(97)00023-6

ELSEVIER

Biochimica et Biophysica Acta 1320 (1997) 195–207

BIOCHIMICA ET BIOPHYSICA ACTA
BBA

Quinone exchange at the A_1 site in Photosystem I in spinach and cyanobacteria

Agnes E. Ostafin *, Stefan Weber

Department of Chemistry, The University of Chicago, 5735 S. Ellis Avenue, Chicago, IL 60637, USA

Received 5 September 1996; revised 23 January 1997; accepted 4 February 1997

Abstract

The electron spin polarization (ESP) EPR signal arising from the P-700$^+$ A_1^- radical pair in Photosystem I (PS I) consisting of the oxidized PS I primary donor, P-700 , and the reduced vitamin K_1 (K_1) acceptor, A_1, is studied as a function of isotopic labelling of the native A_1 acceptor. No pre-extraction of the native A_1 acceptor is utilized, instead, exchange of the native acceptor with protonated or perdeuterated K_1 is accomplished by incubation of the reaction centers in solution (incubation/exchange). The incubation/exchange process is studied in PS I of spinach and in two cyanobacteria, the thermophilic *Synechococcus lividus* (*S. lividus*) and the non-thermophilic *Synechococcus leopoliensis* (*S. leopoliensis*). A complete data set, $^{H}P^{H}A_1$, $^{H}P^{D}A_1$, $^{D}P^{H}A_1$, $^{D}P^{D}A_1$ (where P refers to the primary chlorophyll donor, A_1, the quinone acceptor, and H and D denote protonated and deuterated, respectively), is obtained for *S. lividus*. The correlated radical pair polarization model (CRPP) is used to reproduce the experimental lineshapes for the four different isotopic combinations of the P-700$^+$$A_1^-$ radical pair. The experimental ESP EPR spectra are well predicted using the geometric and energetic parameters which have been deduced for perdeuterated PS I reaction centers in whole cells of *S. lividus* (Kothe, G. et al. (1994) J. Phys. Chem. 98, 2706–2712). The results suggest that the isotopically labelled K_1 binds in the A_1 site with the same orientation as the native acceptor in unexchanged PS I. No evidence for electron transfer to K_1 in configurations other than the A_1 binding site is observed. Incubation/exchange is studied as a function of incubation temperature. For spinach and non-thermophilic *S. leopoliensis* the effect of incubation/exchange is most efficient for 1/2 h incubations at temperatures around and above 30–35°C, but requires somewhat higher incubation temperatures, above 40–45°C, for thermophilic *S. lividus*. Similar changes in the ESP spectrum are also demonstrated for PS I reaction centers in thylakoid membranes of *S. lividus*.

Keywords: Photosystem I; Electron paramagnetic resonance; Electron spin polarization; Vitamin K_1; Quinone exchange; Phylloquinone; A_1 acceptor; Thylakoid

Abbreviations: EPR, electron paramagnetic resonance; ESP, electron spin polarization; LM-EPR, light modulated EPR; PS I, Photosystem I; PS II, Photosystem II; K_1, vitamin K_1; $^{H}A_1$, protonated A_1 quinone acceptor; ^{D}P, perdeuterated primary chlorophyll donor; $^{D}A_1$, perdeuterated A_1 quinone acceptor; ^{H}P, protonated primary chlorophyll donor; Chl_a, chlorophyll a; TX-100, Triton X-100 detergent; CRPP, correlated radical pair polarization; ZQC, zero quantum coherences; fwhm, full width at half maximum; *S. lividus*, *Synechococcus lividus*: *Synechococcus 6717*; *S. leopoliensis*, *Synechococcus leopoliensis*; *Synechocystis PCC 6803*

* Corresponding authors: A.E.O. and S.W. Fax: +1 (773) 702-0805; E-mail: aostafin@rainbow.uchicago.edu and s-weber@uchicago.edu

PII S0005-2728(97)00023-6

1. Introduction

The PS I reaction center in higher plants and cyanobacteria is a membrane-bound pigment-protein complex which facilitates photo-induced electron transfer from plastocyanin to ferredoxin. The primary structure, subunit composition, gene organization, and overall mechanism of PS I function are well conserved throughout evolution [1,2]. Structural details of PS I have been determined at 4.5 Å resolution in a recent X-ray crystallographic study using crystals of trimeric PS I from the thermophilic cyanobacteria *Synechococcus elongatus* [3,4], but the data do not yet allow precise placement of all of the cofactors involved in PS I electron transfer. A heterodimer of two homologous 82–83 kDa polypeptides, PsaA and PsaB, comprises the hydrophobic catalytic core of the PS I reaction center [5–8] and binds accessory antenna chlorophyll molecules, the primary chlorophyll a (Chl_a) electron donor, P-700 , and the electron acceptor cofactors, A_0, A_1, F_x. The PsaA and PsaB proteins are bridged by the 4Fe-4S iron sulfur cluster F_x, via sulfur ligands from cysteine residues. An 8 kDa acidic, hydrophilic protein subunit, PsaC, located at the stromal surface of the core complex [9] binds the terminal 4Fe-4S electron acceptors, F_A and F_B.

The generally accepted path for electron transfer in PS I is P-700 $\rightarrow A_0 \rightarrow A_1 \rightarrow F_x \rightarrow F_{A/B}$ [10]. From the structure at 4.5 Å resolution there is little doubt that P-700 is a chlorophyll dimer [3]. There is evidence that the first electron acceptor, A_0, is also a Chl_a molecule [11,12]. The second electron acceptor, A_1, is phylloquinone, vitamin K_1 (K_1) [13–15]. Electron transfer from the photo-excited primary donor, P-700 , is probably sequential through $A_0 \rightarrow A_1 \rightarrow F_x$, however, it is uncertain whether subsequent electron transfer to $F_{A/B}$ remains sequential [16].

Two molecules of K_1 co-purify per PS I reaction center [17,18]. One K_1 can be removed with hexane, while extraction of the other K_1 requires a slightly more hydrophilic solvent, hexane with 0.3% methanol [17]. In spinach PS I, when phylloquinone is extracted with methanol/hexane solution, the ESP EPR signal observed at low temperature and attributed to $P\text{-}700^+A_1^-$, vanishes [13,19]. Extraction using only hexane does not affect the low-temperature EPR signal [17]. The signal is restored by reconstitution of the PS I reaction center with either protonated or perdeuterated K_1. The ESP EPR signal was also absent in highly reducing conditions under which the A_1 acceptor accepts two electrons [20], but could be restored by removal of the reducing agent by dialysis [13]. Recently, electron transfer to secondary acceptors more electro-positive than A_1 has been observed [21]. However, in the work of Rustandi et al. [19], no spin-polarized EPR signal was found when the A_1 site was reconstituted with quinones that are more electro-positive than the preceeding acceptor (the reduction potential for K_1 is estimated to be ca. -710 mV) [14,19]. Finally, the structure of the reconstituted acceptor seems to require either a minimum of two aromatic rings (i.e., naphthoquinone) or a benzoquinone derivative substituted with an alkyl tail [22]. Related ESP EPR signals have been observerd from PS I where A_1 has been replaced with naphthoquinone or duroquinone (without alkyl tail) but the spectra are noticeably different from that found in native PS I [14,23]. The results from the quinone reconstitution experiments in spinach imply that in order to generate the native ESP EPR signal, the reconstituted quinone must be redox-poised to restore electron transfer activity and also assume a specific orientation in the A_1 site, rather than simply serving as a soluble electron acceptor.

It has been suggested from time-resolved EPR studies that the A_1 in PS I is different from the Q_a binding site in bacterial reaction centers, and that the A_1 quinone acceptor is less tightly bound in the PS I protein matrix [23]. In Rustandi et al. [19], it was reported that replacement of the native quinone in isolated PS I reaction centers does not necessarily require prior chemical extraction, but can occur via an equilibrium exchange process which eliminates the use of solvents that may disturb the native conformational structure of the PS I protein. The equilibrium exchange process involves incubating the isolated PS I reaction centers in the presence of excess quinone until a new equilibrium is established between the concentration of replacement quinone in solution and that bound to the protein at the A_1 site. The extent of quinone exchange depends on incubation conditions. Complete exchange can be accomplished by incubation in the cold overnight, or within

minutes at elevated temperatures (37–50°C), or by illumination during incubation at cold temperatures (5°C) [19].

In this work we examine the observed ESP EPR signal in membrane-bound PS I and isolated PS I in which the A_1 acceptor has been exchanged with an isotopically labelled K_1. The effects of incubation/exchange on the ESP signals in PS I is studied for reaction center particles isolated from spinach, and two cyanobacteria, *S. lividus* (*Synechococcus 6717*), a thermophilic cyanobacteria that grows optimally at 50°C, and a non-thermophilic cyanobacterium, *S. leopoliensis* (*Synechocystis PCC 6803*, formerly *Anacystis nidulans*). In *S. leopoliensis*, A_1 is a 5-monohydroxyphylloquinone, which has a hydroxy group at the C-5 position of the phytyl side chain [24]. The changes in the ESP EPR signals following incubation/exchange are simulated with the CRPP model [25,26] in order to show that the isotopically labeled K_1 binds in the A_1 site with essentially the same geometry as the original acceptor in intact reaction centers [27,28].

2. Materials and methods

Spinach PS I D144 particles were isolated according to the procedures of Anderson and Boardman [29]. Perdeuterated *S. leopoliensis* and perdeuterated and protonated *S. lividus* were grown as described previously [30], and PS I particles from these cyanobacteria were prepared according to the procedures of Biggins and Mathis [18]. Isolated PS I particles were suspended in 50 mM Tris buffer (pH 7.5) with 0.2% Triton X-100 (TX-100) and centrifuged to remove insoluble material. In all cases 2 mM sodium ascorbate was added to the preparation. Protonated K_1 was obtained from Aldrich and used without further purification. Perdeuterated K_1 was extracted from perdeuterated *S. lividus*, purified by HPLC, and its purity verified by absorption spectroscopy and desorption mass spectroscopy as described previously [13].

Exchange of the A_1 acceptor in the solubilized perdeuterated and protonated PS I particles was accomplished by incubating each in the presence of an excess of protonated or perdeuterated K_1. A final concentration of 50–300 μM K_1 in 250 μl of TX-100 solubilized PS I solution diluted to a final absorbance of 15–20 A.U./cm at 670 nm was used. No additional effort was made to further purify the PS I proteins to remove excess quinone following solubilization in TX-100. To ensure uniform dispersion of added quinone in the PS I solutions, the added vitamin K_1 was either premixed to form a 2% ethanol solution, or dispersed in a small amount of Tris buffer/10% TX-100 solution (Tiede, D., private communication). When ethanol was used as the dispersant, the final TX-100 concentration was 0.2%, and when 10% TX-100 was used, the final detergent concentration was 0.24%. Control samples contained no added quinone, only the same volume of dispersing medium (e.g., ethanol or TX-100) as the equivalent quinone-containing sample.

PS I samples were incubated with an excess concentration of the isotopically labelled K_1 as a function of: (1) temperature between 4°C and 50°C; (2) concentration of excess quinone between 0 and 300 μM; and (3) incubation time between 1/2 and 24 h. For each experimental measurement, both a PS I preparation and a control sample were incubated at the same temperature for an identical time interval. To check for artifacts in the ESP EPR spectrum arising from temperature-dependent conformations of the reaction center protein, EPR samples frozen immediately following the 1/2 h incubation period at liquid nitrogen temperatures (−196°C) were compared with samples re-equilibrated at 4°C on ice for at least 20 min. before freezing in liquid nitrogen.

Intact thylakoid membrane fractions were obtained by sonication of whole cells of *S. lividus* in Tris buffer. After centrifugation to remove unbroken cells, the thylakoid fractions were suspended in buffer with excess ascorbic acid, and incubated in the presence of excess protonated K_1 at 10°C for 24 h. The K_1 was solubilized in a small amount of TX-100/buffer solution for uniform dispersal. EPR X-band measurements were performed on either a Varian E-9 spectrometer system, or Bruker ESP300E system, equipped with an Air Products low-temperature accessory. Light-induced EPR signals were generated with a 300 W xenon arc lamp (ILC technologies), with wavelength components below 400 nm and above 1000 nm eliminated with an aqueous sodium nitrite solution filter.

ESP EPR spectra were recorded using the light

modulated EPR (LM-EPR) technique [31] in which the EPR signal is detected with respect to both the 100 kHz field modulation and the electronically modulated light intensity (reference wave function provided by a Wavetek Model 180 function generator). A light modulation frequency, ω_L, in the range of 500 Hz was used. The signal obtained via phase-sensitive detection with respect to ω_L is the first harmonic component of the EPR signal. Phase-sensitive detection and signal amplification was done using a PAR EG&G 5208 lock-in amplifier referenced to the modulation light source. Lock-in amplifier phase angles were adjusted to maximize the $P\text{-}700^+A_1^-$ radical pair ESP EPR signals observed in control samples. By optimizing the phase/frequency parameters of our lock-in detector, we preferentially detect EPR signals from the incubation/exchange sample which are coherently in phase relative to the control sample, and filter out any irreversible (on the timescale of ω_L) EPR signals. All spectra were recorded at a temperature of about 13 K. Simulations of the ESP EPR signals were carried out with FORTRAN programs [32] developed to implement the CRPP [25,26].

3. Results

3.1. Temperature dependence of quinone exchange in PS I particles from spinach and cyanobacteria

The changes in spin-polarized EPR lineshape as a function of incubation temperature are presented in Fig. 1 and Fig. 2. No significant change in ESP EPR lineshape relative to the control sample was observed for samples incubated without added K_1 at any incubation temperature. The ESP EPR spectra from protonated spinach D144 particles which have been incubated with 100 μM of perdeuterated K_1 for a 1/2 h interval at 5°C, 20°C, 30°C, 40°C and 50°C, as well as a control sample which was not incubated are shown in Fig. 1A. The control and 5°C ESP EPR signals are relatively weak in intensity and possess the rather broad lineshape features characteristic of a fully protonated PS I reaction center. After 1/2 h incubation at 20°C in the presence of 100 μM of perdeuterated K_1, the spin-polarized EPR signal is increased in intensity and the absorptive and emissive features within the spectrum narrow slightly. Following incubations at 30°C and above, the resultant ESP EPR signal shows greater increase in intensity and narrowing of spectral features. Between 30°C and 40°C, the intensity increase and spectral narrowing of the ESP EPR spectrum following incubation reaches a limit, and additional 1/2 h incubations at 50°C do not change the lineshape, nor affect the intensity of the observed ESP EPR signal.

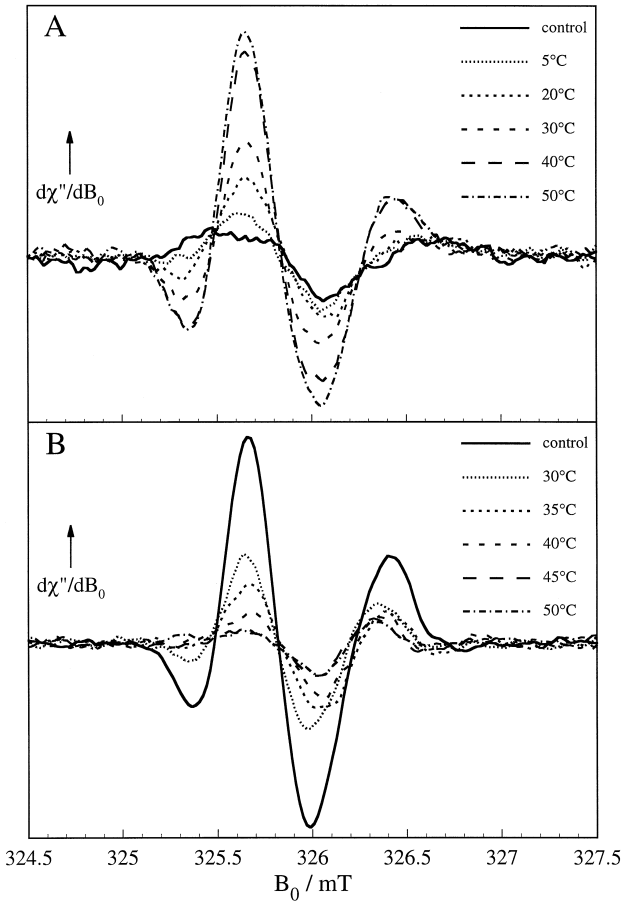

Fig. 1. A: ESP EPR signals from spinach D144 particles in Tris buffer (pH 7.5) in 0.2% Triton X-100, with 2 mM ascorbic acid and 100 μM 2% ethanol/perdeuterated vitamin K_1 as a function of incubation temperature. B: ESP EPR signals from perdeuterated *S. leopoliensis* particles in Tris buffer (pH 7.5) in 0.2% Triton X-100, with 2 mM ascorbic acid and 100 μM perdeuterated vitamin K_1 as a function of incubation temperature. Spectra shown are derivative $d\chi''/dB_0$ of the absorption mode signal. Microwave frequency 9.142 GHz, microwave power 2 mW, 0.1 mT G modulation amplitude, X-band spectra are taken at 13 K.

The spin-polarized EPR spectra for perdeuterated *S. leopoliensis* PS I particles, similarly incubated for 1/2 h intervals at a series of temperatures between

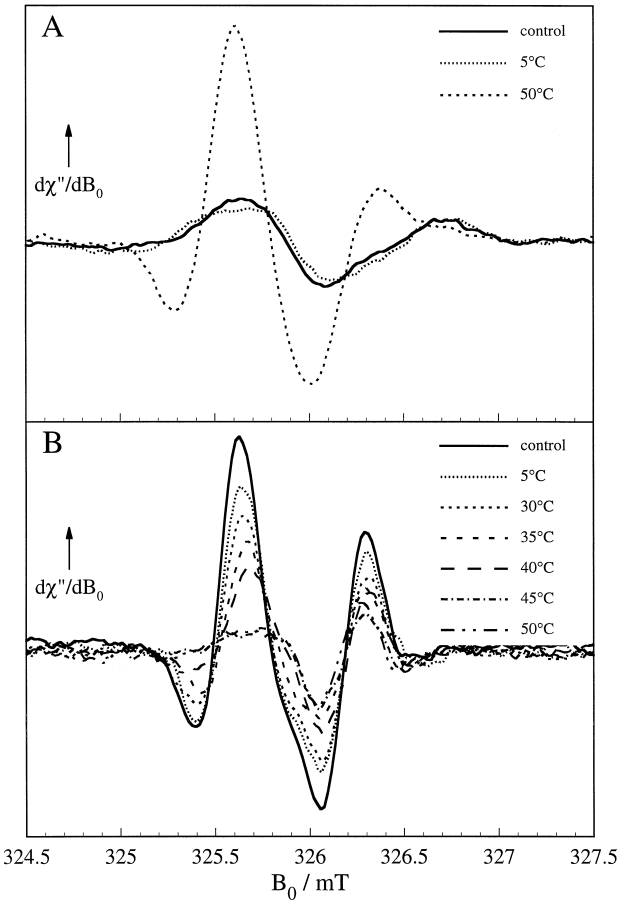

Fig. 2. ESP EPR signals from (A) protonated and (B) perdeuterated *S. lividus* in Tris buffer (pH 7.5) in 0.2% Triton X-100, with 2 mM ascorbic acid and 100 μM of A) 2% ethanol/perdeuterated vitamin K_1, or B) 2% ethanol/protonated vitamin K_1 as a function of incubation temperature. Spectra shown are derivative $d\chi''/dB_0$ of the absorption mode signal. Microwave frequency 9.142 GHz, microwave power 2 mW, 0.1 mT modulation amplitude, X-band spectra are taken at 13 K.

30°C and 50°C in the presence of 100 μM protonated K_1, are presented in Fig. 1B. In this case, the initially intense narrow ESP EPR signal, characteristic of a fully deuterated PS I reaction center, decreases in intensity, and obvious broadening of the spectral features is observed following 1/2 h incubations above 30°C. As with spinach PS I particles, the magnitude of these spectral changes is largest for 1/2 h incubations at temperatures above 30°C. After 1/2 h incubation at temperatures above 45°C, no further changes in the ESP signal are observed. Additional 1/2 h incubations at 50°C did not affect the spectrum either.

The case of protonated *S. lividus* PS I particles, incubated for 1/2 h intervals in the presence of 100 μM perdeuterated K_1 are presented in Fig. 2A. A significant narrowing of features and increase in intensity of the spin-polarized EPR signal is observed following 1/2 h incubation at elevated temperature. Two samples, incubated at 5°C and 50°C are shown to demonstrate that the EPR lineshape changes are nearly identical with the changes observed in spinach PS I particles incubated with excess K_1 (Fig. 1A).

The changes for the spin-polarized EPR spectrum for perdeuterated *S. lividus* PS I particles, incubated for 1/2 h intervals in the presence of 100 μM protonated K_1 are presented in Fig. 2B. For 1/2 h incubations at temperatures between 5°C and 50°C, the initially intense, narrow ESP EPR signal characteristic of a fully deuterated PS I reaction center is decreased in intensity, with a simultaneous broadening in spectral features. The spectral changes are nearly identical with those observed in perdeuterated *S. leopoliensis* incubated over the same temperature range (Fig. 1B), except for a small shift in the temperature at which the spectral changes appear to be complete following the 1/2 h incubation period. For incubations at temperatures above 45°C no further change in the EPR signal is observed. Incubation for 1/2 h at 50°C, as well as additional 1/2 h incubations at 50°C, do not affect the ESP spectrum.

The typically observed P-700$^+$ EPR linewidth was ca. 0.4 mT for perdeuterated PS I control samples, and ca. 0.75 mT for fully protonated PS I control samples (data not shown). For samples incubated at temperatures between 5°C and the temperature beyond which no further change in the ESP EPR lineshape is observed, linewidth and signal intensity are intermediate between the two extremes. No difference in results were obtained using the two methods of quinone dispersion (ethanol solubilized K_1, or TX-100 suspended K_1).

4. Discussion

4.1. CRPP model simulations of the ESP EPR signals from PS I samples incubated at 50°C

The ESP EPR signal for perdeuterated and fully protonated PS I particles of *S. lividus*, and perdeuter-

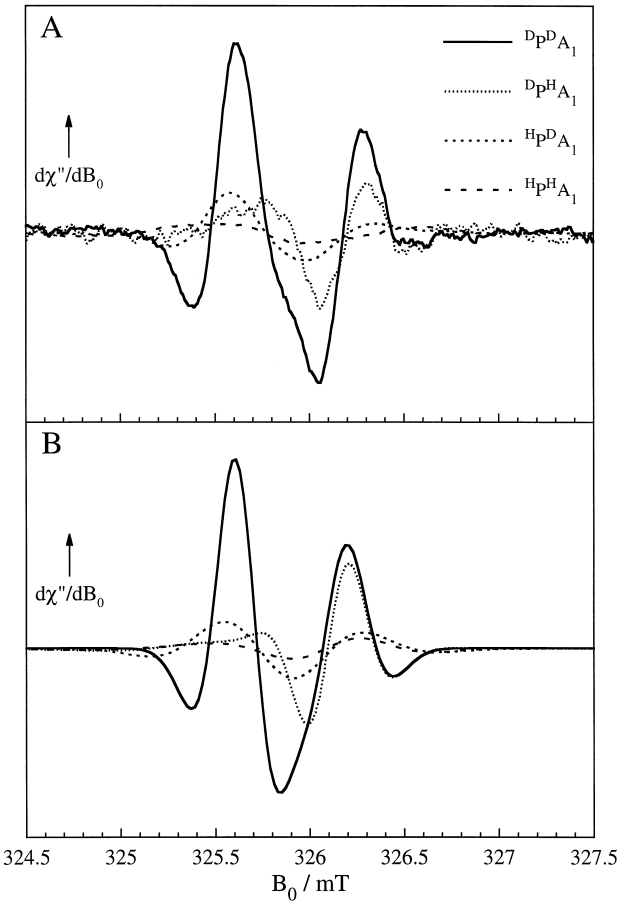

Fig. 3. A: Light modulation ESP EPR (LM-EPR) spectra for the four isotopically mixed cases for P-700^{+}A$_1^{-}$ in isolated *S. lividus* PSI particles. Mixed variants were prepared via incubation/exchange method. Microwave frequency 9.142 GHz, microwave power 2 mW, 0.1 mT modulation amplitude, X-band spectra are taken at 13 K. B: correlated radical pair polarization (CRPP) model calculations for the four isotopically mixed cases for P-700^{+}A$_1^{-}$ in PS I.

ated and protonated PS I particles incubated for a 1/2 h at 50°C in the presence of an excess concentration of protonated and perdeuterated K_1, respectively, are reproduced in Fig. 3A. They are labeled $^{D}P^{D}A_1$, $^{H}P^{H}A_1$ and $^{D}P^{H}A_1$, $^{H}P^{D}A_1$, where P denotes the primary donor P-700 , A_1 the secondary electron acceptor, and the superscripts D and H refer to the corresponding perdeuterated and protonated species, respectively. The spectra shown were obtained as the derivative $d\chi''/dB_0$ of the absorption mode EPR signal.

Model calculations based on the CRPP mechanism for the four radical pair cases $^{D}P^{D}A_1$, $^{H}P^{H}A_1$, $^{D}P^{H}A_1$, and $^{H}P^{D}A_1$ are presented in Fig. 3B as the derivative $d\chi''/dB_0$ of the signal with respect to the magnetic field. The basics of the CRPP model have been described elsewhere [25,26]. The CRPP model is applicable to a spin-correlated radical pair, created in either a singlet or triplet configuration (i.e., created directly from an excited singlet or triplet state precursor) which is not an eigenstate of the radical pair Hamiltonian. The ESP evolves as a function of the magnetic interactions between the two separated spins and nearby nuclei. The implementation of the CRPP model used in this analysis [32] evaluates the observable of the radical pair Hamiltonian in which the magnetic interactions between electron and nuclear spins are included explicitly. A static (stick) spectrum defined by the *g*-tensors, electron-electron spin interactions, and isotropic hyperfine couplings in the radical pair is generated. Inhomogeneous linebroadening is included via a Gaussian spin-packet on each hyperfine component of the spectrum.

Listed in Table 1 are the parameters used in the CRPP model simulations shown in Fig. 3B. We have assumed for the purpose of simulation that in all cases the incubated and exchanged samples have the same cofactor geometry as found in native PS I from perdeuterated whole cells. This mutual orientation geometry for the P-700^{+}A$_1^{-}$ radical pair is adapted from a least-squares fit of the short-time spin dynamics in time-resolved transient EPR (including transient nutations and zero quantum precessions) [28,33] from PS I reaction centers in whole cells of perdeuterated *S. lividus*. The phase and the frequency of the high-frequency signal modulations are a unique signature of the magnetic interactions within the P-700^{+}A$_1^{-}$ radical pair.

To simulate the expected EPR signals, the second moments of the ESP EPR lineshapes for the four cases $^{D}P^{D}A_1$, $^{H}P^{H}A_1$, $^{D}P^{H}A_1$, and $^{H}P^{D}A_1$, were evaluated by expressing the total second moment $\langle H^2 \rangle$ as a sum of contributions from hyperfine-interacting nuclei, $\langle H^2 \rangle_{HFS}$, plus an additional term $\langle H^2 \rangle_{res}$, which encompasses all other inhomogeneous contributions to the EPR lineshape (such as residual hyperfine interactions and *g* strain) that are not included in the definition of the orientation-dependent spin Hamilton operator

$$\langle H^2 \rangle = \langle H^2 \rangle_{HFS} + \langle H^2 \rangle_{res} \quad (1)$$

Table 1
Parameters used in model calculations for the light-induced radical pairs $P\text{-}700^{+}A_1^{-}$ in *S. lividus*

g-Tensors [a]			Geometry [a]			Second moments	Spin–spin interaction [a]	
	$P\text{-}700^{+}$	A_1^{-}		$P\text{-}700^{+}$	$\boldsymbol{D}$	$P\text{-}700^{+H}$	A_1^{-H}	
g_{xx}:	2.00304	2.00564	φ:	$-15°$	0°	$\langle H^2\rangle_{HFS}^{P\text{-}700^{+}} = 4.39\cdot10^{-2}\ mT^{2D}$	$\langle H^2\rangle_{HFS}^{A_1^{-}} = 1.15\cdot10^{-1}\ mT^{2D}$	$J = 0$
g_{yy}:	2.00262	2.00494	ϑ:	28°	58°	$\langle H^2\rangle_{HFS}^{P-700^{+}} = 2.77\cdot10^{-3}\ mT^{214N}$	$\langle H^2\rangle_{HFS}^{A_1^{-}} = 7.29\cdot10^{-3}\ mT^{2H}$	$D = -0.12$ mT
g_{zz}:	2.00232	2.00217	ψ:	27°	$-1°$	$\langle H^2\rangle_{HFS}^{P-700^{+}} = 1.07\cdot10^{-2}\ mT^{2}$	$\langle H^2\rangle_{HFS}^{Matrix} = 4.21\cdot10^{-2}\ mT^{2D}$	
							$\langle H^2\rangle_{HFS}^{Matrix} = 2.66\cdot10^{-3}\ mT^{2res}$	
							$\langle H^2\rangle_{HFS}^{Matrix} = 3.00\cdot10^{-3}\ mT^{2}$	
+						$\langle H^2\rangle_{res} = 4.60\cdot10^{-3}\ mT^{2}$		

[a] Data taken from [28]. The Euler angles φ, ϑ and ψ relate the principal axis system of the respective magnetic tensor (*g*-tensor of $P\text{-}700^{+}$, dipolar coupling tensor $\boldsymbol{D}$) and the molecular reference system (*g*-tensor of A_1^{-}).

with

$$\langle H^2\rangle_{\mathrm{res}} = \frac{1}{8\ln 2}\cdot \Delta B_{1/2}^2 \qquad (2)$$

and

$$\langle H^2\rangle_{\mathrm{HFS}} = \sum_i \tfrac{1}{3} I_i(I_i+1)a_i^2 \qquad (3)$$

Here, I_i is the nuclear spin quantum number of the ith nucleus and a_i is its isotropic hyperfine coupling constant [34].

The magnitude of $\langle H^2\rangle_{\mathrm{res}}$ used in our calculations ($\langle H^2\rangle_{\mathrm{res}} = 4.6\cdot 10^{-3}$ mT^2) corresponds to a Gaussian with a full width at half maximum of $\Delta B_{1/2} =$ 0.16 mT, and is in good agreement with values used in simulations of transient EPR spectra and time profiles of perdeuterated whole cells *S. lividus* [28]. For P-700$^+$ the hyperfine contribution $\langle H^2\rangle_{\mathrm{HFS}}^{\text{P-700}^+}$ to the total second moment $\langle H^2\rangle^{\text{P-700}^+}$ can be divided into two parts

$$\langle H^2\rangle_{\mathrm{HFS}}^{\text{P-700}^+} = {}^{14\mathrm{N}}\langle H^2\rangle_{\mathrm{HFS}}^{\text{P-700}^+} + {}^{\mathrm{H\,or\,D}}\langle H^2\rangle_{\mathrm{HFS}}^{\text{P-700}^+} \qquad (4)$$

due to couplings of the unpaired electron spin with nitrogens and either protons (H) or deuterons (D). The primary donor P-700 is a dimer of Chl$_a$ molecules with a very asymmetric electronic structure of P-700 , where the electron spin resides mainly on one of the dimer halves [35,26]. A summary of the EPR evidence for and against a symmetric charge distribution is given in a recent review [37]. Recently, electron-nuclear double resonance (ENDOR) and electron spin-echo envelope modulation (ESEEM) experiments on ^{15}N-enriched P-700$^+$ have been performed, and five ^{15}N hyperfine coupling tensors could be identified [36]. It was even possible to distinguish larger nitrogen couplings from smaller ones that possibly arise from the second dimer half contributing only weakly to the pair. In our calculations we use ${}^{14\mathrm{N}}\langle H^2\rangle_{\mathrm{HFS}}^{\text{P-700}^+} = 1.07\cdot 10^{-2}$ mT^2 for the second moment arising from the hyperfine couplings of the ^{14}N nuclei ($I=1$) in the Chl$_a$ species. This value has been estimated from the hyperfine pattern of the ^{15}N nuclei ($I=1/2$) in P-700$^+$ [36] using the quotient of the gyromagnetic ratios of the two nitrogen isotopes ^{14}N and ^{15}N: ${}^{14\mathrm{N}}\gamma/{}^{15\mathrm{N}}\gamma = 0.713$.

For the case of protonated P-700$^+$ the second moment contribution due to protons ${}^{\mathrm{H}}\langle H^2\rangle_{\mathrm{HFS}}^{\text{P-700}^+}$ is estimated using the isotropic average of the couplings of the three distinct methyl groups in Chl$_a$ of P-700$^+$ obtained by ^{1}H-ENDOR [38]. The sum contribution of protons to the total second moment is ${}^{\mathrm{H}}\langle H^2\rangle_{\mathrm{HFS}}^{\text{P-700}^+} = 4.39\cdot 10^{-2}$ mT^2. For deuterated P-700$^+$ the deuteron couplings were obtained from the proton hyperfine couplings using the relation ${}^{\mathrm{H}}\gamma/{}^{\mathrm{D}}\gamma = 6.514$, thus yielding ${}^{\mathrm{D}}\langle H^2\rangle_{\mathrm{HFS}}^{\text{P-700}^+} = 2.77\cdot 10^{-3}$ mT^2. Therefore, the ratio of the total second moments of protonated and deuterated P-700$^+$ is $\langle H^2\rangle^{\mathrm{H}\text{P-700}^+}/\langle H^2\rangle^{\mathrm{D}\text{P-700}^+} = 3.28$. This value corresponds to a ratio of linewidths of protonated versus deuterated P-700$^+$ of 1.81, which is close to the experimentally observed ratio of 1.89. It is noteworthy, that the total second moment of $\langle H^2\rangle^{\mathrm{D}\text{P-700}^+} = 1.81\cdot 10^{-2}$ mT^2 is in fair agreement with the value used to simulate the zero-quantum precessions in transient EPR [28].

For the photo-accumulated radical state of the PS I secondary electron acceptor A$_1$, A$_1^-$, in *Anabaena variabilis* an inhomogeneous linewidth of 0.95 mT has been reported [39,40]. Significantly smaller linewidths of 0.86 mT and 0.833 mT were observed in W-band EPR studies of reduced protonated K$_1$, K$_1^-$, in frozen solutions of protonated and perdeuterated isopropanol, respectively [41]. Therefore we conclude, that an additional broadening due to the interaction of the immobilized phylloquinone radical A$_1^-$ with the large biopolymer matrix has to be taken into account for a simulation of the X-band ESP EPR spectra of quinone exchanged PS I. This conclusion is corroborated by the fact that incubation of ${}^{\mathrm{H}}\mathrm{P}{}^{\mathrm{H}}\mathrm{A}_1$ with ${}^{\mathrm{D}}\mathrm{K}_1$ (${}^{\mathrm{H}}\mathrm{P}{}^{\mathrm{H}}\mathrm{A}_1 \rightarrow {}^{\mathrm{H}}\mathrm{P}{}^{\mathrm{D}}\mathrm{A}_1$) yields an ESP EPR spectrum which is considerably broader (in the region where the A$_1^-$ resonances occur) than that of ${}^{\mathrm{D}}\mathrm{P}{}^{\mathrm{D}}\mathrm{A}_1$. Likewise, incubation of ${}^{\mathrm{D}}\mathrm{P}{}^{\mathrm{D}}\mathrm{A}_1$ with ${}^{\mathrm{H}}\mathrm{K}_1$ (${}^{\mathrm{D}}\mathrm{P}{}^{\mathrm{D}}\mathrm{A}_1 \rightarrow {}^{\mathrm{D}}\mathrm{P}{}^{\mathrm{H}}\mathrm{A}_1$) results in an EPR spectrum which is narrower than the spectrum of ${}^{\mathrm{H}}\mathrm{P}{}^{\mathrm{H}}\mathrm{A}_1$. Therefore, we account for matrix effects by adding a term $\langle H^2\rangle_{\mathrm{HFS}}^{\mathrm{Matrix}}$ for A$_1^-$

$$\langle H^2\rangle_{\mathrm{HFS}}^{\mathrm{A}_1^-} = {}^{\mathrm{H\,or\,D}}\langle H^2\rangle_{\mathrm{HFS}}^{\mathrm{A}_1^-} + \langle H^2\rangle_{\mathrm{HFS}}^{\mathrm{Matrix}} \qquad (5)$$

with

$$\langle H^2\rangle_{\mathrm{HFS}}^{\mathrm{Matrix}} = {}^{\mathrm{H\,or\,D}}\langle H^2\rangle_{\mathrm{HFS}}^{\mathrm{Matrix}} + {}^{\mathrm{res}}\langle H^2\rangle_{\mathrm{HFS}}^{\mathrm{Matrix}} \qquad (6)$$

Here, ${}^{\mathrm{H\ or\ D}}\langle H^2\rangle_{\mathrm{HFS}}^{\mathrm{Matrix}}$ describes hyperfine contributions to the second moment due to hydrogen or deuteron bonds from the matrix protein to the quinone.

The term ${}^{res}\langle H^2\rangle_{HFS}^{Matrix}$ encompasses all other inhomogeneous contributions due to effects from nuclei other than protons or deuterons in the protein matrix. We have estimated ${}^{H}\langle H^2\rangle_{HFS}^{A_1^-}$ using averaged values for the hyperfine interactions of the 2-methyl protons and β-methylene protons in the phytyl side chain of A_1^- in *A. variabilis* obtained from ^{1}H-ENDOR and electron-nuclear-nuclear TRIPLE resonance spectroscopy [40] to be ${}^{H}\langle H^2\rangle_{HFS}^{A_1^-} = 1.15 \cdot 10^{-1}$ mT^2. Using reported values for the hyperfine couplings assigned to protons in the protein matrix hydrogen-bonded to both carbonyl oxygens of A_1^- we obtain ${}^{H}\langle H^2\rangle_{HFS}^{Matrix} = 4.21 \cdot 10^{-2}$ mT^2. A residual contribution ${}^{res}\langle H^2\rangle_{HFS}^{Matrix} = 3.0 \cdot 10^{-3}$ mT^2 implies that also nuclei within the protein matrix other than protons add to the A_1^- linewidth. The latter component was estimated based on a comparison between calculated and experimental ESP EPR spectra of P-700$^+$A$_1^-$. A possible source for this additional broadening, which is independent on the protonation or deuteration of the A_1^- surrounding, are nitrogen nuclei nearby the quinone phenolate oxygens of the A_1^- acceptor of the PS I reaction center. We obtain ${}^{D}\langle H^2\rangle_{HFS}^{A_1^-} = 7.29 \cdot 10^{-3}$ mT^2 and ${}^{D}\langle H^2\rangle_{HFS}^{Matrix} = 2.66 \cdot 10^{-3}$ mT^2 from a simple scale-down using the relation ${}^{H}\gamma/{}^{D}\gamma = 6.514$. The total second moments for A_1^- in the four cases considered are $\langle H^2\rangle^{DA_1^-} = 1.76 \cdot 10 - 2$ mT^2 in ^{D}P^{D}A$_1$, $\langle H^2\rangle^{DA_1^-} = 5.70 \cdot 10^{-2}$ mT^2 in ^{H}P^{D}A$_1$, $\langle H^2\rangle^{HA_1^-} = 1.25 \cdot 10^{-1}$ mT^2 in ^{D}P^{H}A$_1$, and $\langle H^2\rangle^{HA_1^-} = 1.65 \cdot 10^{-1}$ mT^2 in ^{H}P^{H}A$_1$.

The experimental and simulated ESP EPR signals in Fig. 3A,B do not exactly overlap. Optimization of the simulation parameters by fitting to the experimental data would certainly improve their agreement. Since we have no a priori knowledge of how to additionally modify the simulation parameters, we have used the spectra in Fig. 3B to demonstrate that we can obtain correct relative lineshape changes among the four cases using reasonable estimates for the second moments. We are well aware that most of the hyperfine couplings on the P-700$^+$ halve [36,42] as well as on the quinone halve [40] of the radical pair are anisotropic in nature. However, in most of the cases, the main axes of the hyperfine coupling tensors with respect to the main axes of the g matrices and the axis that connects the two radical pair halves are not yet known. In light of this, it seems that the calculation of ESP EPR spectra using second moments of line patterns from isotropic hyperfine couplings is justified given the present state of knowledge.

The zero field splitting and electron-spin exchange parameters, $D = -0.12$ mT, and $J = 0$, used in the present calculations are identical to those proposed by Stehlik et al. [43]. Some discussions about the distance of the two radical pair halves in PS I and hence, the strength of the electron–electron spin interaction have been triggered by the recent low-resolution X-ray diffraction studyof PS I at 4.5 Å resolution [3,4]. A somewhat larger value for the dipolar spin interaction parameter D was suggested based on the analysis of an out-of-phase electron spin-echo and its echo envelope modulation (ESEEM) measured in a two-pulse EPR experiment with PS I particles from *Synechococcus elongatus* [44,45]. That, and a very recent re-evaluation of the g-tensor anisotropy of A_1^- [46] leads to the conclusion that the proposed geometry of the secondary radical pair P-700$^+$A$_1^-$ [27,28], which was obtained based on fixed values of magnetic interaction parameters from older work, needs a minor refinement. However, it is not the purpose of this paper to make a regression fit of the experimental spectra in order determine geometries, but rather to demonstrate that, for the four cases generated via incubation/exchange, essentially the same parameter set can be used to approximate the experimentally obtained data. From this we conclude that the incubation/exchange procedure has not significantly changed the geometry of the secondary radical pair in the four cases considered.

In the CRPP model simulations shown in Fig. 3B, the possibility of differences in the g tensor anisotropy of K_1 among the four isotopically mixed cases was not considered. By changing the g factor anisotropy it is possible to improve the CRPP model simulation of the ESP EPR spectra (data not shown). Similar improved agreement of simulation with experiment could not be achieved by changing the average hyperfine coupling alone, and suggests that a change in the g tensor anisotropy of A_1^- occurs when protonated K_1 is exchanged into perdeuterated reaction centers and when perdeuterated K_1 is exchanged into protonated reaction centers. The apparent requirement for a change in g tensor anisotropy in order to better approximate the experimental ESP EPR spectra could be related to differences in hydro-

gen bonding strength of the phenolate oxygens of K_1 when bound to protonated or perdeuterated PS I protein. Hydrogen bonding with the quinone phenolate oxygen, at least in semiquinone systems, has been suggested to be stronger with protons than deuterons (equilibrium constant $K_{H/D}$ is 5.8 in methanol below -120°C) [47,48]. A decreased *g* anisotropy compared to solution values is expected when K_1 is bonded strongly because a shift in electron density away from the phenolate oxygens occurs [23]. Thus, a smaller *g* anisotropy is expected when K_1 is H-bonded to a protonated PS I protein ($^{H}P^{H\,(or\ D)}A_1$) compared to a D-bonded perdeuterated PS I protein ($^{D}P^{H(or\ D)}A_1$).

The effect of hydrogen bonding has similarly been invoked recently [23] to explain differences in the magnitude of *g*-tensor anisotropy between protonated PS I and bacterial reaction centers reconstituted at the A_1 site with K_1, ubiquinone, duroquinone and naphthoquinone acceptors. In particular, the g_{xx} and g_{yy} components of the K_1 *g*-tensor in reconstituted PS I were even larger than that measured in frozen alcohol solution [41], and the actual observed linewidth of the reconstituted PS I samples was larger than what would be predicted using solvent *g*-tensors.

4.2. Electron transfer to the A_1 electron acceptor following exchange at 50°C in S. lividus

Each curve in Fig. 3A represents the final state of PS I reaction centers following incubation/exchange (i.e., 1/2 h incubation at 50°C). Since all four isotopic mixtures of exchanged PS I particles can be simulated using essentially the same geometric parameters to describe the P-700$^+$A$_1^-$ pair, which furthermore, are identical to those deduced for native PS I reaction centers in whole cells of *S. lividus*, we conclude that the exchanged isotopically labeled K_1 has replaced the native A_1 acceptor, and resides in essentially the same orientation with similar magnetic interaction with the primary donor cation P-700$^+$. The electron transfer characteristics of the native and exchanged PS I samples should be similar as well. Reversible electron transfer to K_1 not in the A_1 binding site is not likely on the time scale of normal electron transfer reactions in native PS I. One would expect that adventitiously absorbed K_1 would create radical pairs with a random geometry and dipolar interaction as compared with the homogeneous population of P-700$^+$A$_1^-$ pairs in the native PS I particle. On the other hand, if K_1 binds specifically to a site other than the A_1 site, these parameters would be non-random, but different from those in native PS I. In either case, the ESP EPR signals are expected to be quite different from native PS I, because the spin dynamics of the radical pair system would be altered.

Preliminary time-resolved EPR measurements of native and exchanged PS I samples at room temperature indicate that the $\approx$ 200 ns lifetime of P-700$^+$A$_1^-$ is not altered following quinone exchange. This, together with the good agreement of the CRPP model simulations described above, suggests that not only does the exchanged K_1 occupy the A_1 site in essentially the same geometry, but also functions effectively in electron transfer.

4.3. Comparison of the temperature dependence of exchange in PS I from spinach, S. leopoliensis, and S. lividus

We have demonstrated that the exchange of the A_1 acceptor is possible in PS I particles derived from spinach and from cyanobacteria (Fig. 1 and Fig. 2). The effect of incubation temperature on the effectiveness of exchange with an isotopically labelled K_1, is presented for PS I derived from spinach (Fig. 1A), perdeuterated *S. leopoliensis* (Fig. 1B), and protonated (Fig. 2A) and perdeuterated (Fig. 2B) *S. lividus*. The PS I sources we have used have different optimal growing temperatures. Spinach and the non-thermophilic *S. leopoliensis* grow well at ambient temperatures (ca. 21°C), while the thermophilic *S. lividus* at relatively high temperatures (ca. 50°C).

Assuming that the low-field and center-field portions of the spin-polarized EPR spectrum are proportional to the extent of replacement of native quinone via the exchange procedure, a qualitative comparison of the results between the three sources of PS I reaction centers can be made. A trend is observed in the effect of incubation temperature on the intensity of the center-field portion of the ESP EPR spectrum. Beginning with the control sample, the intensity of this spectral feature varies continuously with increasing incubation temperature, down to smaller intensity in the case of spinach, and up to larger intensity for the initially perdeuterated cyanobacteria, until some

temperature beyond which the intensity remains relatively constant. A large jump in signal intensity is seen at 30°C for spinach, 35°C for *S. leopoliensis*, and 45°C for *S. lividus*. These jumps in PS I from spinach, *S. leopoliensis* and *S. lividus* appear to correspond to their relative optimal growing temperatures. This correspondence may be related to the different lipids and proteins that determine the thermal characteristics of these organisms. The different native phylloquinone acceptor in the A_1 site in the case of *S. leopoliensis* (5-monohydroxyphylloquinone) may also have a distinct exchange temperature dependence. More work is necessary to fully understand these issues.

4.4. Exchange in PS I-containing thylakoids of S. lividus

The first ESP EPR signals from exchanged perdeuterated thylakoid structures derived from perdeuterated *S. lividus* are shown in Fig. 4. Thylakoids were incubated with 1.57 mM protonated K_1 at 10°C for 24 h. The ESP EPR lineshape change, following incubation of thylakoids in the presence of excess K_1, is similar to what was observed in nearly completely exchanged isolated PS I reactions centers derived from perdeuterated *S. leopoliensis* and *S. lividus*.

The success of exchange in PS I reaction centers which have not been isolated from the thylakoid membrane has an intriguing implication. It suggests that the binding of the A_1 electron acceptor in PS I is weak enough to permit displacement by other quinone-like molecules, without the need for elevated temperature incubation. Thus, the A_1 site could be targeted as a herbicide binding site [19]. The fact that exchange of the A_1 acceptor is possible for low-temperature incubation (4° C) of PS I-containing thylakoids can be accomplished is a promising step.

Whether the quinone exchange discussed in this work has physiological importance remains to be understood. A physiological role for a labile quinone is known in PS II reaction centers of higher plants and cyanobacteria. In this case, following double-reduction, the secondary quinone Q_B in PS II reaction centers is able to diffuse from the core reaction center complex as plastoquinol QH_2. Another quinone, from the plastoquinone pool which is located within the

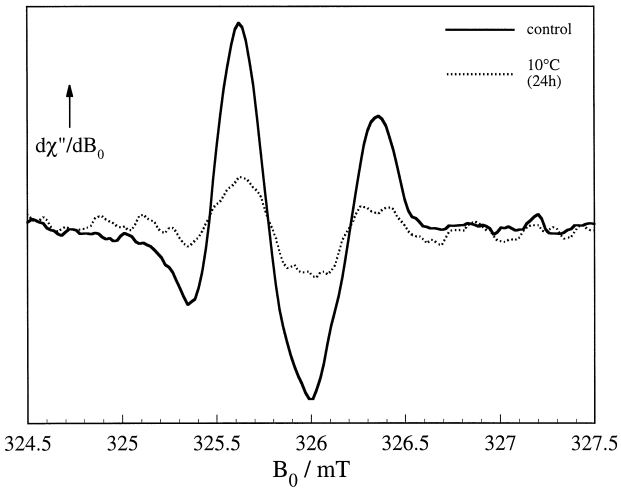

Fig. 4. Light modulation ESP EPR (LM-EPR) spectra in thylakoids of *Synechococcus lividus* incubated overnight at 10°C, with and without 1.57 μM protonated vitamin K_1. Spectra shown are derivative $d\chi''/dB_0$ of the absorption mode signal.Microwave frequency 9.142 GHz, microwave power 2 mW, 0.1 mT modulation amplitude, X-band spectra are taken at 13 K.

thylakoid membrane diffuses in to take its place. The liberated QH_2 serves as an electron donor to the cytochrome b_6/f complex which in turn catalyzes the oxidation of plastoquinol, and the reduction of plastocyanin. Plastocyanin is the principle reductant of P-700 , the primary electron donor in the light-driven reactions of the PS I reaction center.

The primary activity of the PS I reaction center is somewhat different. The known physiological function of PS I is to produce NADPH via a ferredoxin-NADP reductase which is bound to the stromal side of the thylakoid membrane (non-cyclic electron transport). Electron microscopy and crystallography studies have suggested that several of these surface-exposed proteins PsaC, PsaD, and PsaE may be part of the ferredoxin docking site [49]. Electron transfer from the primary donor P-700 appears to proceed through a series of electron acceptors, terminating in $F_X/F_A/F_B$ complex, adjacent to ferredoxin-NADP reductase. The NADPH-producing non-cyclic electron transport mechanism is supplemented by a cyclic process in which the ferredoxin instead transfers the electron back to the cytochrome b_6/f complex. The net result of both mechanisms is an electrochemical proton gradient which is coupled to ATP synthesis and respiration. The mechanistic details of the cyclic

electron transport are unclear, and perhaps a labile quinone in the PS I complex could play a role in this mechanism. However, there is no evidence at this time on which to base such a conclusion. As discussed earlier, in PS I the phylloquinone vitamin K_1, is found in a stoichiometric ratio of 2:1 [17,18]. There does not appear to be a phylloquinone pool analogous to the intra-membrane plastoquinone pool associated with PS II.

The apparently more weakly bound PS I reaction center quinone (removable with hexane) is not the A_1 acceptor detected in the EPR experiment [13,17,19], and which we believe to be exchanged with isotopically labeled K_1 in these experiments. Although we have verified that the observed changes in the EPR signal are the same with ethanol-solubilized and detergent suspended K_1, it is entirely possible that the protein conformation and local environment near the quinone to be polar enough to loosen the binding site. In the isolated thylakoids, we did not make any efforts to maintain an isotonic solution, thus a partially damaged membrane (perhaps with the ferredoxin docking proteins removed) might have allowed the quinone exchange process to occur accidentally, and not necessarily be a physiological process. The slower exchange at 4°C required much longer time to effect the same extent of change in the EPR spectrum, and over time diffusion of water and salts may result in some protein unfolding which exposes the A_1 binding site. Such a partial loosening is also probably occurring at elevated temperatures. In order to answer those questions it is necessary to make a systematic study of preparation conditions and their effect on the exchange process. Thus, it is premature to speculate about a possible physiological role for quinone exchange in PS I.

5. Conclusions

Incubation of solubilized PS I reaction centers derived from spinach, perdeuterated non-thermophilic cyanobacterium *S. leopoliensis*, and both protonated and perdeuterated thermophilic cyanobacterium *S. lividus* with an excess of isotopically labelled vitamin K_1 results in characteristic lineshape changes in the ESP EPR signal of the P-700$^+$ A_1^- radical pair. These changes can be simulated using the CRPP model using geometric and energetic parameters adapted from studies of whole cells of PS I-containing *S. lividus*. The good agreement of simulated EPR signals with the experiment implies that the exchange procedure replaces the native A_1 acceptor with isotopically labelled K_1 in essentially the same geometry, preserving the overall characteristic interaction with the binding pocket and with its interacting radical partner P-700$^+$.

There appears to be no evidence for electron transfer from P-700 to K_1 adventitiously bound to the PS I protein. The fact that substitution of the native quinone A_1 acceptor with an isotopically labelled vitamin K_1 can be accomplished in isolated PS I particles without prior chemical extraction of the native acceptor, and also in intact thylakoid membrane fractions, is suggestive of a relatively accessible A_1 acceptor binding site in the PS I unit. The physiological function of this accessibility is not yet understood. The exchange effect is studied as a function of incubation temperature for spinach, *S. leopoliensis*, and *S. lividus* PS I. The efficiency of exchange appears to follow a trend in which exchange is more efficient at lower temperatures for spinach, and requires higher temperatures for cyanobacteria, particularly for the thermophilic *S. lividus*. Similarities in the ESP signals observed among the three PS I sources spinach, *S. leopoliensis*, and *S. lividus*, before and after exchange of the A_1 acceptor, demonstrate the generality of the exchange procedure.

Acknowledgements

The authors would like to thank Dr. Seth W. Snyder, Aaron Barkoff and Nicole Brunkan for initial experimental observation of temperature and concentration dependencies and preliminary computer modeling, Dr. Melanie M. Werst for sample preparation and verification of initial EPR studies, and Dr. Marion C. Thurnauer, Dr. Jau Tang, Dr. James R. Norris, Dr. Phil Laible, and Dr. Lisa M. Utschig for helpful discussion. Experimental work was completed during the postdoctoral appointment of A.E.O. at Argonne National Laboratory, under the financial support by the U.S. Department of Energy, Office of Basic Sciences (Contract W-31-109-ENG-38) which is

gratefully acknowledged. S.W. thanks the Alexander von Humboldt Foundation (Bonn, Germany) for the award of a Feodor Lynen Fellowship.

References

[1] J.H. Chitnis, Q. Xu, V.P. Chitnis, R. Nechushtai, Photosynth. Res. 43 (1995) 23–40.
[2] J.H. Golbeck, Proc. Natl. Acad. Sci. USA 90 (1993) 1642–1646.
[3] N. Krauß, W.D. Schubert, O. Klukas, P. Fromme, H.T. Witt, W. Saenger, Nature Struct. Biol. 3 (1996) 965–973.
[4] N. Krauß, W. Hinrichs, I. Witt, P. Fromme, W. Pritzkow, Z. Dauter, C. Betzel, K.S. Wilson, H.T. Witt, W. Saenger, Nature 361 (1993) 326–331.
[5] S.M. Rodday, R. Schulz, L. McIntosh, J. Biggins, Photosynth. Res. 42 (1994) 185–190.
[6] S.M. Rodday, S.S. Jun, J. Biggins, Photosynth. Res. 36 (1993) 1–9.
[7] J.H. Golbeck, Annu. Rev. Plant Physiol. Plant Mol. Biol. 43 (1992) 293–324.
[8] L.E. Fish, U. Kück, L. Bogorad, J. Biol. Chem. 260 (1985) 1413–1421.
[9] D.A. Bryant (1992) in The Photosystems: Structure, Function and Molecular Biology (Barber, J., Ed.), Ch. 13, pp. 501–545, Elsevier Science, Amsterdam.
[10] J.H. Golbeck, D.A. Bryant, Curr. Topics Bioenerg. 16 (1992) 83–177.
[11] J. Bonnerjea, M.C.W. Evans, FEBS Lett. 148 (1982) 313–316.
[12] P. Gast, T. Swarthoff, F.C.R. Ebskamp, A.J. Hoff, Biochim. Biophys. Acta 722 (1983) 163–175.
[13] R.R. Rustandi, S.W. Snyder, L.L. Feezel, T.J. Michalski, J.R. Norris, M.C. Thurnauer, Biochemistry 29 (1990) 8030–8032.
[14] I. Sieckmann, A. van der Est, H. Bottin, P. Setif, D. Stehlik, FEBS Lett. 284 (1991) 98–102.
[15] S.W. Snyder, R.R. Rustandi, J. Biggins, J.R. Norris, M.C. Thurnauer, Proc. Natl. Acad. Sci. USA 88 (1991) 9895–9896.
[16] B. Guigliarelli, J. Guillaussier, C. More, P. Setif, H. Bottin, P. Bertrand, J. Biol. Chem. 268 (1993) 900–908.
[17] R. Malkin, FEBS Lett. 208 (1986) 343–346.
[18] J. Biggins, P. Mathis, Biochemistry 27 (1988) 1494–1500.
[19] R.R. Rustandi, S.W. Snyder, J. Biggins, J.R. Norris, M.C. Thurnauer, Biochim. Biophys. Acta 1101 (1992) 311–320.
[20] P. Setif, H. Bottin, Biochemistry 28 (1989) 2689–2697.
[21] M. Iwaki, S. Kumazaki, K. Yoshihara, T. Erabi, S. Itoh (1995) in Photosynthesis: From Light to Biosphere, Vol. II (P. Mathis, Ed.), pp. 147–150, Kluwer Academic, Dordrecht.
[22] J. Biggins, Biochemistry 29 (1990) 7259–7264.
[23] A. van der Est, I. Sieckmann, W. Lubitz, D. Stehlik, Chem. Phys. 194 (1995) 349–359.
[24] K. Ziegler, I. Maldener, W. Lockau, Z. Naturforsch. 44c (1989) 468–472.
[25] C.D. Buckley, D.A. Hunter, P.J. Hore, K.A. McLauchlan, Chem. Phys. Lett. 135 (1987) 307–312.
[26] G.L. Closs, M.D.E. Forbes, J.R. Norris, J. Phys. Chem. 91 (1987) 3592–3599.
[27] M. Gierer, A. van der Est, D. Stehlik, Chem. Phys. Lett. 186 (1991) 238–247.
[28] G. Kothe, S. Weber, E. Ohmes, M.C. Thurnauer, J.R. Norris, J. Phys. Chem. 98 (1994) 2706–2712.
[29] J.M. Anderson, N.K. Boardman, Biochim. Biophys. Acta 112 (1966) 403–421.
[30] H.F. DaBoll, H.L. Crespi, J.J. Katz, Biotechn. Bioeng. 4 (1962) 281–297.
[31] H. Levanon, S. Vega, J. Chem. Phys. 61 (1974) 2265–2274.
[32] S. Weber (1994) PhD thesis, Universität Stuttgart.
[33] G. Kothe, S. Weber, R. Bittl, E. Ohmes, M.C. Thurnauer, J.R. Norris, Chem. Phys. Lett. 186 (1991) 474–480.
[34] C.P. Poole, Electron Spin Resonance: a Comprehensive Treatise on Experimental Techniques. John Wiley, New York, 2nd edn., 1983.
[35] I.H. Davis, P. Heathcote, D.J. MacLachlan, M.C.W. Evans, Biochim. Biophys. Acta 1143 (1993) 183–189.
[36] H. Käß, W. Lubitz, Chem. Phys. Lett. 251 (1996) 193–203.
[37] A. Angerhofer, R. Bittl, Photochem. Photobiol. 63 (1996) 11–38.
[38] H. Käß (1995) PhD thesis, Technische Universität, Berlin.
[39] P. Heathcote, J.A. Hanley, M.C.W. Evans, Biochim. Biophys. Acta 1144 (1993) 54–61.
[40] S.E.J. Rigby, M.C.W. Evans, P. Heathcote, Biochemistry 35 (1996) 6651–6656.
[41] O. Burghaus, M. Plato, M. Rohrer, K. Möbius, F. MacMillan, W. Lubitz, J. Phys. Chem. 97 (1993) 7639–7647.
[42] H. Käß, E. Bittersmann-Weidlich, L.E. Andreasson, B. Bönigk, W. Lubitz, Chem. Phys. 194 (1995) 419–432.
[43] D. Stehlik, C.H. Bock, J. Petersen, J. Phys. Chem. 93 (1989) 1612–1619.
[44] S. Zech, W. Lubitz, R. Bittl, Ber. Bunsenges. Phys. Chem. 100 (1996) 2041–2044.
[45] R. Bittl, S. Zech (1997) J. Phys. Chem. B, in press.
[46] A. van der Est, T. Prisner, R. Bittl, P. Fromme, W. Lubitz, K. Möbius, D. Stehlik (1997) J. Phys. Chem. B, in press.
[47] B.J. Hales, E.E. Case, Biochim. Biophys. Acta 637 (1981) 291–302.
[48] R.W. Mansfield, J.H.A. Nugent, M.C.W. Evans, Biochim. Biophys. Acta 894 (1987) 515–523.
[49] P. Fromme, W.D. Schubert, N. Krauß, Biochim. Biophys. Acta 1187 (1994) 99–105.